doi: 10.18323/2782-4039-2025-3-73-10

Strength of joints produced by ultrasonic spot welding of copper plates using tools with different tooth heights

Elvina R. Shayakhmetova, junior researcher
Institute for Metals Superplasticity Problems of RAS, Ufa (Russia)

E-mail: elvinar@imsp.ru ORCID: https://orcid.org/0000-0002-1659-9922

Received 30.06.2025 *Revised 21.07.2025* *Accepted 12.08.2025*

Abstract: Ultrasonic welding of metals is an energy-efficient, environmentally friendly technology that allows producing solid-state joints between thin blanks. The widespread use of this technology is hampered by the low strength of the resulting joints and the instability of their properties. One of the ways to improve strength characteristics is to develop a welding tool that ensures stable transmission of ultrasonic vibration energy to the joint zone. For this purpose, a relief with teeth or pyramids of different shapes and heights is applied to the surface of the welding tip and anvil. This paper presents data on the fracture load and fracture energy of lap joints produced by ultrasonic spot welding of copper plates using tools with a tooth height of 0.1 and 0.4 mm. Ultrasonic welding was carried out with a frequency of 20 kHz and a vibration amplitude of 18–20 μm, the welding duration was 2 and 3 s, the clamping force was 2.5 kN. The paper considers the features of the fracture of the produced joints and the distribution of normal strains in the weld spot, and results of calculation of stress intensity factors in its vicinity. It is shown that after ultrasonic welding for 3 s, the strength characteristics of the joints produced with different tools reach the highest values, they are close in magnitude, but the experimental data scatter is half as much after welding with a tool with small teeth. The joints produced with such a tool fractured along the interface of the joint, and after welding with a tool with large teeth, the fracture developed with nugget pull-out, which is explained by an increase in the stress intensity factor at the tip of the concentrator surrounding the weld spot.

Keywords: copper; ultrasonic welding of metals; solid-state joint; joint strength; welding tool relief; stress intensity factor.

Acknowledgments: This work was carried out within the state assignment of IMSP RAS (No. 124022900006-2). Part of experimental data was obtained during the accomplishment of a project supported by the Russian Science Foundation (grant No. 22-19-00617, https://rscf.ru/project/22-19-00617/). Electron microscopic studies and mechanical tests were carried out on the facilities of shared services center of IMSP RAS “Structural and Physical-Mechanical Studies of Materials”.

The author expresses deep gratitude to M.A. Murzinova, PhD (Engineering), and A.A. Nazarov, Doctor of Sciences (Physics and Mathematics), for their assistance in conducting the research and a discussion of the results obtained.

The paper was written on the reports of the participants of the XII International School of Physical Materials Science (SPM-2025), Togliatti, September 15–19, 2025.

For citation: Shayakhmetova E.R. Strength of joints produced by ultrasonic spot welding of copper plates using tools with different tooth heights. *Frontier Materials & Technologies*, 2025, no. 3, pp. 125–136. DOI: 10.18323/2782-4039-2025-3-73-10.

INTRODUCTION

Ultrasonic welding (USW) of metals is an energy-efficient, environmentally friendly technology used primarily to produce electrical contacts in the automotive and electrical industries [1]. Currently, the USW method is used to produce joints of metal blanks made of sheets, tapes, foils, and wires with a cross-section of up to 3 mm.

Despite a number of advantages, the widespread use of ultrasonic welding of metals is limited due to the low strength of the resulting joints and the wide scatter of mechanical test results [2; 3]. This is largely associated with the small magnitude and uneven distribution of strains over the area of the weld spot, which are necessary to form and increase the area of microwelds [4; 5].

The distribution and magnitude of strain depend on the temperature in the joint zone, the thickness of the welded blanks, their thermophysical and mechanical properties, and conditions of USW, primarily, the input welding energy, which is proportional to the time of USW, and the compressive pressure [6–8]. At the selected pressure at initial stages of ultrasonic welding, the upper plate should slide over the lower one, ensuring the removal of oxide films and contaminants from contacting surfaces, as well as their heating due to friction. At final stages of the process, the same pressure should be sufficient to heal discontinuities in the joint zone of metals heated to 0.4–0.8 of melting temperature [1; 3].

To transmit the ultrasonic vibration energy from the sonotrode to the joining zone, knurls of different shapes

and depths are applied to the surface of the welding tip and anvil [1; 9–11]. A relief formed by pyramids or teeth, the height and periodicity of which amount fractions of a millimeter, is created on the tool surface. The penetration of teeth/pyramids into the blanks to be joined ensures their contact with the tool, but is accompanied by extrusion of the metal into the valleys on the tool surface. As a result, the distribution of strains in the weld spot area becomes periodic [1; 5; 11].

In [5], a clear correlation was found between the distribution of normal strains in the central cross section of the weld spot and the linear weld density. In the described experiments, a satisfactory density of at least 70 % was observed in those areas where the sample was subjected to compression by 15 % or more. At the same time, in neighbouring areas, where the metal was extruded into the tool valleys, tensile strains were recorded, and the linear weld density decreased to 5 %. Compressive strains sufficient for healing defects can be achieved after the tool teeth completely penetrated into the surface of the plates being joined and the valleys are completely filled with metal [4], which can lead to an increase in the strength of the joints. One can expect that with a decrease in the height of the teeth, their penetration into the surface of the plates will occur faster, and, all other conditions being equal, the USW sample in the weld spot will experience compressive strains sufficient to form high-strength welded joints.

The aim of this work is to analyse the reasons for changes in the fracture load and the fracture mode of copper lap joints produced by ultrasonic spot welding using a tool with different tooth heights.

METHODS

The experiments were performed on copper plates with dimensions 50×20 mm^2 cut from 0.8 mm thick sheets manufactured by LLC Degtyarsk Metallurgical Plant, Yekaterinburg (Russia). The chemical composition of the sheets, specified in the manufacturer’s certificate, is presented in Table 1.

Before welding, the plates were ground on abrasive paper of P240 grit at an angle of 45° to the long side of the plate and degreased with alcohol and acetone. Such preparation allows distinguishing reliably traces of sliding that occur during ultrasonic welding and scratches that appear during mechanical tests on the fracture surfaces from traces of preliminary surface treatment of the plates.

Ultrasonic welding was performed on a laboratory facility manufactured at the Institute for Metals Superplasticity Problems of the Russian Academy of Sciences (Russia) and successfully used in welding titanium [12], nickel [13], and copper [14] plates. Welding tips with identical sizes, 6×6 mm^2, and a relief in the form of teeth of different heights were used: H=0.4 mm and H=0.1 mm (Fig. 1). The relief of the anvil corresponded to the relief of the tip. Hereinafter in the text, the tool with a tooth height of H=0.1 mm is called the tool with small teeth or fine ones,

Table 1. *Chemical composition of the investigated material according to GOST 859-2014, wt. %*
Таблица 1. *Химический состав исследованного материала по ГОСТ 859-2014, мас. %*

Cu	O	Zn	Fe	Pb	S	Ni	Others
99.96	0.02	0.004	0.003	0.003	0.002	0.001	<0.03

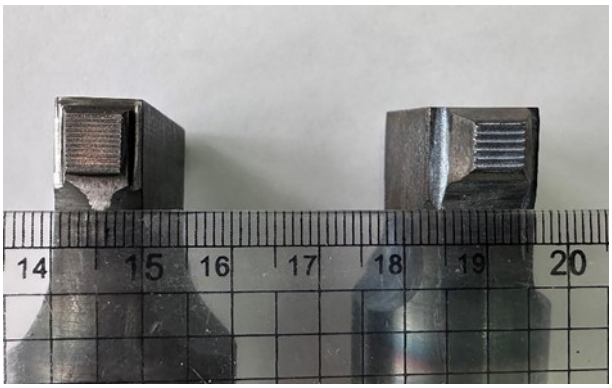

Fig. 1. *Photograph of welding tips used in ultrasonic welding:*
on the left – a tip with teeth of H=0.1 mm, on the right – with teeth of H=0.4 mm
Рис. 1. *Фотография сварочных наконечников, использованных при УЗС:*
слева – наконечник с зубцами H=0,1 мм, справа – с зубцами H=0,4 мм

and the tool with a tooth height of H=0.4 mm is called the tool with large teeth or coarse ones.

Ultrasonic welding was performed with a frequency of 20 kHz and a vibration amplitude of the sonotrode of 18–20 μm. The direction of vibrations was parallel to the short side of the plates. The clamping force was 2.5 kN, the time of ultrasound exposure was 2 and 3 s.

The strength properties of the joints were assessed based on the results of tensile lap shear tests in accordance with the recommendations of GOST 6996-66. The tests were carried out on an Instron 5982 universal testing machine (England) at room temperature with a crosshead speed of 1 mm/min. During the tests, the crosshead displacement (l, mm) and the corresponding loading force (F, N) were recorded. The maximum (peak) value F=F_{max} was considered the sample fracture load. The area under the $F(l)$ curve limited by the F_{max} value was taken as the fracture energy of the joints (A, J). The average values of fracture load ($\bar{F}_{max}$) and the fracture energy ($\bar{A}$) of joints produced by ultrasonic welding with different tools for each mode were obtained based on the test results of at least 4 samples. The standard deviation was taken as the value of statistical error.

The fracture surfaces of the tested samples were examined on a TESCAN MIRA 3 LMH FEG scanning electron microscope (Czech Republic) in the secondary electron mode at magnifications from ×20 to ×2000.

The depth of penetration of the tip teeth was measured on an instrumental microscope in the central section of the weld spot parallel to the direction of vibration of the tip. When performing the measurements, the coordinates of the centre of the imprint of each tooth and the tip valley (x_i; y_i), as well as the thickness of the welded sample at this point (h_i) were recorded. The magnitude of the normal strain of the sample (e_{ni}, %) at each point was calculated as e_{ni}=100×(h_i–h_0)/h_0, where h_0 is the thickness of the two initial plates. Based on the calculation results, distributions of normal strains and the depth of penetration of the tool teeth in the central section of the welded sample were constructed. The technique for these measurements and the construction of distributions of normal strains of the sample is described in detail and illustrated in [5]. Additionally, the depth of penetration of the teeth was measured in the peripheral sections of the weld spots, as well as by the imprints of the tips on the welded samples, recording the change in the focal length when focusing on the surface of the plate and the bottom of the imprint of each tooth. The measurements performed showed that the depth of penetration of the teeth decreased equally in the directions parallel and perpendicular to the tip vibration.

RESULTS

Mechanical tests

Changing the height of the tool teeth does not significantly affect the fracture load and fracture energy of the joints produced under the same USW conditions (Table 2). However, the scatter of experimental values of $\bar{F}_{max}$ and $\bar{A}$ is twice as large after welding with the coarse tool. All samples produced by USW for 2 s fractured along the interface of the joint (Fig. 2 a). Increasing the welding time from 2 to 3 s did not change the type (mode) of fracture of the samples produced with the tool with small teeth, but caused an increase in the values of $\bar{F}_{max}$ and $\bar{A}$ (Table 2).

In contrast, increasing the time of welding with the tool with large teeth did not affect $\bar{F}_{max}$ and $\bar{A}$ of the joints, but led to a change in their fracture mode, which occurred with a partial nugget pull-out of the weld spot (Fig. 2 b, c). The crack initiated on the side of the weld spot perpendicular to the direction of the tensile force and propagated along this side. Further fracture of the samples occurred in different ways. In some cases, the crack extended beyond the weld spot and grew in the plate, opening under the action of the tensile load (Fig. 2 b). In this case, the free edges of the plates were bent around the weld spot. In other cases, the crack continued to propagate along the sides of the spot,

Table 2. *Properties of joints of copper plates produced by ultrasonic welding with a tool with different tooth heights*
Таблица 2. *Свойства соединений пластин меди, полученных УЗС инструментом с разной высотой зубцов*

Properties of joints	Teeth height (H); USW time (t)			
	H=0.1 mm; t=2 s	H=0.1 mm; t=3 s	H=0.4 mm; t=2 s	H=0.4 mm; t=3 s
$\bar{F}_{max}$, N	1593±101	2075±100	1814±294	1918±241
k_F, %	6	5	16	12
$\bar{A}$, J	0.46±0.18	1.76±0.61	0.99±0.64	1.91±1.06
k_A, %	39	34	64	66
Fracture mode	Interface fracture			Nugget pull-out

Note. $\bar{F}_{max}$ is average values of fracture load; k_F is a coefficient of variation of experimental $\bar{F}_{max}$ values; $\bar{A}$ is average values of fracture energy; k_A is a coefficient of variation of experimental $\bar{A}$ values.

Примечание. $\bar{F}_{max}$ – средние значения усилий разрушения; k_F – коэффициент вариации экспериментальных значений $\bar{F}_{max}$; $\bar{A}$ – средние значения работы разрушения; k_A – коэффициент вариации экспериментальных значений $\bar{A}$.

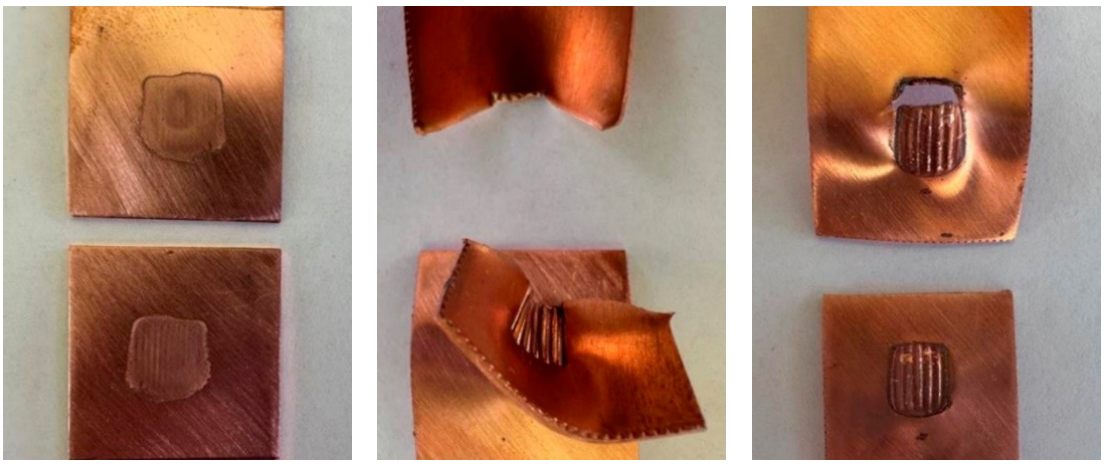

a *b* *c*

Fig. 2. *Photographs of samples after testing:*
a *– interfacial fracture;* ***b***, ***c*** *– partial nugget pull-out fracture*
Рис. 2. *Фотографии образцов после испытаний:*
a *– разрушение по поверхности соединения;* ***b***, ***c*** *– разрушение с частичным отрывом сварной точки*

parallel to the tensile force. However, the closure of the cracks growing towards each other was not observed. It was preceded by bending of the free edges of the plates and fracture along the interface of the joint (Fig. 2 c).

Fractographic analysis

In all cases, the fracture surface had a wavy macrorelief created by the teeth of the welding tool (Fig. 3 a, c and 4 a, c). The features of the microrelief under the tooth imprints and between them depended on the USW time and the height of the teeth.

On the fracture surfaces of the samples welded with a tool with small teeth (H=0.1 mm) for 2 s, a uniform microrelief is observed, the height of the irregularities of which is comparable to the depth of the scratches from preliminary grinding (Fig. 3 b). Both under the tooth imprints and between them, small dimples are observed, slightly elongated in the direction of the tip vibration. On the fracture surfaces of these samples, neither microwelds with a developed dimple microrelief nor areas with smoothed tops of scratches from preliminary grinding are observed, which indicates tight contact of the plates during ultrasonic welding. After welding with the same tool for 3 s, under the imprints of all the teeth there are microwelds consisting of many dimples elongated in the direction of shear (Fig. 3 d).

The microrelief on the fracture surfaces of samples produced with the tool with a tooth height of H=0.4 mm is very heterogeneous. After welding for 2 s, numerous microwelds are observed under the tooth imprints, while traces of preliminary grinding are observed between them (Fig. 4 b). In these areas, the tops of the scratches from preliminary grinding are crushed (smoothed), and there are almost no areas with small dimples. Increasing the USW time to 3 s leads to a significant expansion of the areas occupied by microwelds and to the appearance of a microrelief with small dimples between the tooth imprints in the areas where traces of preliminary grinding are preserved (Fig. 4 d).

Results of measuring normal strains

The noted features of the location of microwelds on the fracture surfaces are associated with different distributions of strains in the weld spots, which, in turn, largely depend on the penetration of the tool teeth into the joined plates. The tip teeth with a height of H=0.1 mm penetrated into the welded plate relatively uniformly over the entire area of the weld spot to a depth of 0.07–0.08 mm after USW for 2 s (Fig. 5 a). After USW for 3 s, the relief height on the plate surface reached 0.1 mm, and the size of the weld spot reached the size of the welding tip (Fig. 5 a, c). Along the entire cross-section of the weld spot, compressive strains were observed, the value of which reached 12 % under the tooth imprints and decreased to 3 % under the tip valleys (Fig. 5 b, blue line). It is evident that the normal strains of the sample varied according to a periodic law. The period value is uniquely determined by the distance between the tool tooth tops and is 0.6 mm for a tool with H=0.1 mm.

The depth of penetration of the coarse tip teeth (H=0.4 mm) was noticeably greater in the centre of the weld spot and decreased toward its periphery (Fig. 5 a, d, e). After ultrasonic welding for 2 and 3 s, the greatest penetration depth in the centre of the weld spot was 0.25 and 0.37 mm, respectively, and the smallest one at the periphery of the spot was 0.17 and 0.28 mm. Since the tip teeth were not completely penetrated into the plate surface, the weld spot size remained smaller than the size of the welding tip. The period of change in normal strains of the samples welded with the tool with a tooth height of H=0.4 mm was 0.9 mm, which corresponds to the distance between the tool tooth tops. In this case, periodically changing compressive strains of 7–14 % across the entire cross-section of the weld spot (Fig. 5 b, red solid line) were observed if the tip teeth were located above the anvil valleys, as shown in Fig. 5 d. With any other relative position of the tool teeth and valleys (Fig. 5 e), compressive strains were replaced by tensile strains (red dotted line in Fig. 5 b). In the absence of control

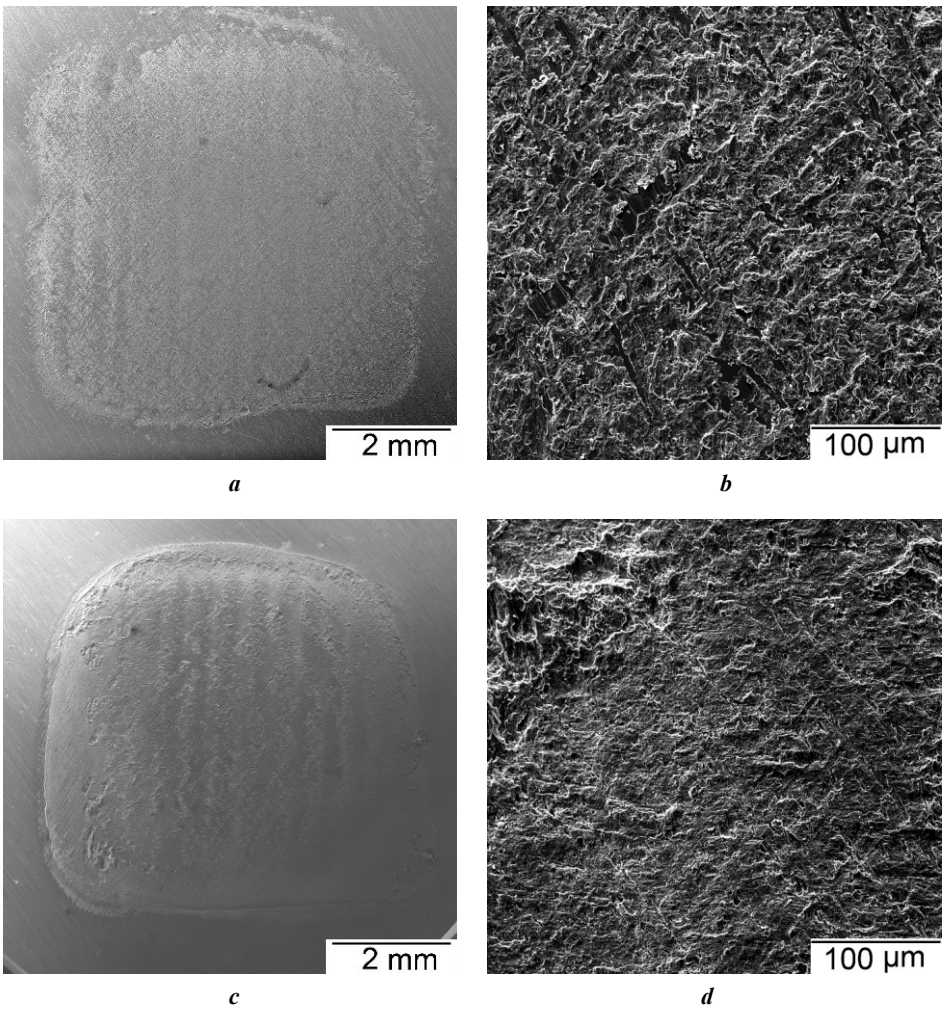

Fig. 3. *Typical images of fracture surfaces of samples produced by ultrasonic welding with a tool with a tooth height of H=0.1 mm:*
a, ***b*** *– welding time of 2 s;* ***c***, ***d*** *– welding time of 3 s;* ***a***, ***c*** *– macrorelief;* ***b***, ***d*** *– microrelief*
Рис. 3. *Типичные изображения поверхностей разрушения образцов, полученных УЗС инструментом с высотой зубцов H=0,1 мм:*
a, ***b*** *– время воздействия ультразвука 2 с;* ***c***, ***d*** *– время воздействия ультразвука 3 с;*
a, ***c*** *– макрорельеф;* ***b***, ***d*** *– микрорельеф*

over the relative position of the 0.4 mm high tool teeth, the distribution of strains in the samples produced under the same welding conditions differed significantly, which caused a significant scatter in the fracture load value.

DISCUSSION

Tensile shear tests are the simplest and therefore the most common method for assessing the quality of spot welded joints. The value of $\bar{F}_{\max}$ characterises the load-bearing capacity of welded samples, and the value of $\bar{A}$ characterises their ability to resist elastic and plastic deformations [1]. At the same time, the question of the sufficiency of these data for assessing the performance of joints and the possibility of comparing strength characteristics remains debatable.

It follows from the data obtained that under the selected USW conditions, the use of a welding tool with a tooth height of 0.1 and 0.4 mm allows producing joints of copper plates with a thickness of 0.8 mm, which demonstrate the same (within the statistical error) values of fracture load and fracture energy. In this case, the scatter of experimental data is half as much after welding with a tool with 0.1 mm high teeth.

During ultrasonic welding, teeth with a height of H=0.1 mm completely penetrate into the joined plates, which ensures 1) the occurrence of normal compressive strains at the weld spot; 2) equality of the weld spot dimensions to the dimensions of the welding tip; 3) reduction in the thickness of the plates at the weld spot periphery by no more than 0.1 mm.

With an uncontrolled mutual arrangement of the teeth of the welding tip and anvil with a height of H=0.4 mm, their incomplete/partial penetration into the plate caused 1) the occurrence of both compressive and tensile normal strains at the weld spot, which is consistent with the results of work [5]; 2) the formation of a weld spot whose size is smaller than the tip size; 3) a reduction in the thickness of the plates at the weld spot periphery by 0.17–0.28 mm.

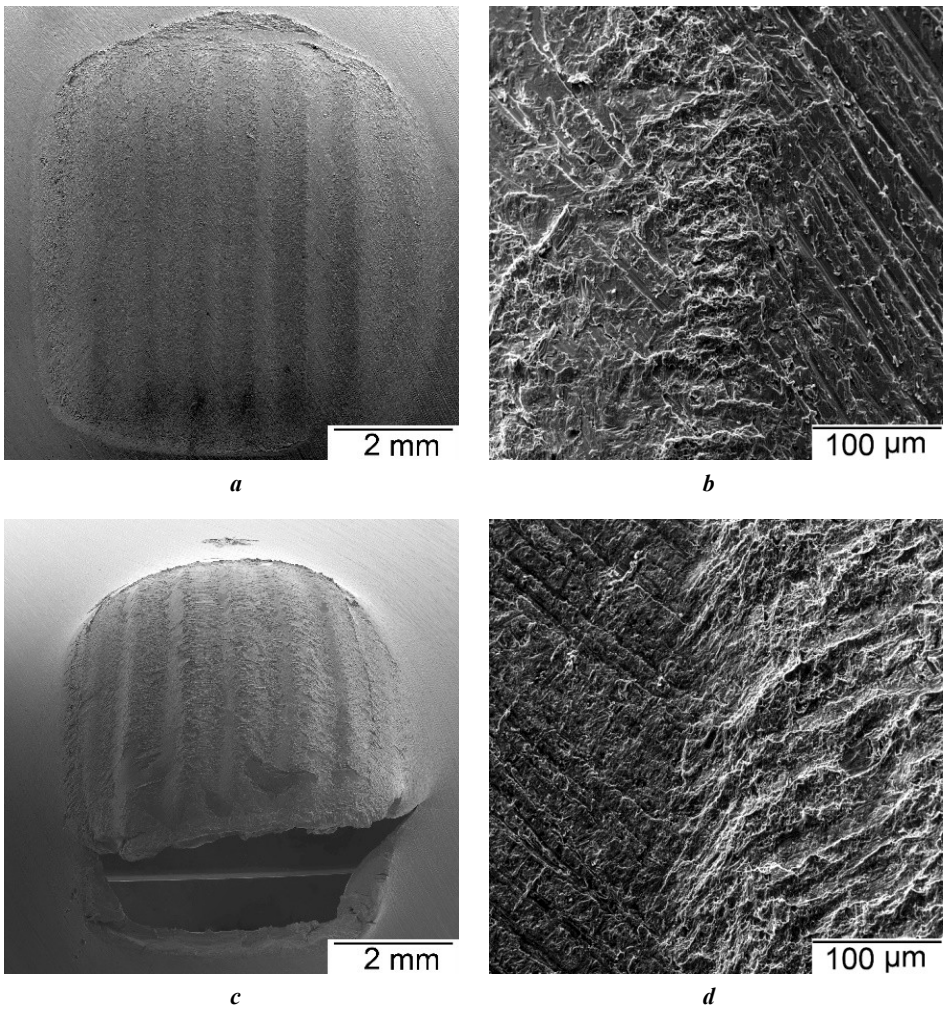

Fig. 4. *Typical images of fracture surfaces of samples produced by ultrasonic welding with a tool with a tooth height of H=0.4 mm:*
a, ***b*** *– welding time of 2 s;* ***c***, ***d*** *– welding time of 3 s;* ***a***, ***c*** *– macrorelief;* ***b***, ***d*** *– microrelief*
Рис. 4. *Типичные изображения поверхностей разрушения образцов, полученных УЗС инструментом с высотой зубцов H=0,4 мм:*
a, ***b*** *– время воздействия ультразвука 2 с;* ***c***, ***d*** *– время воздействия ультразвука 3 с;* ***a***, ***c*** *– макрорельеф;* ***b***, ***d*** *– микрорельеф*

Due to the difference in the sizes of the weld spots (Fig. 5), the comparison of the $\bar{F}_{\max}$ values (Table 2) becomes not entirely correct. The results of assessment of the weld joint strength σ as the ratio of $\bar{F}_{\max}$ to the weld spot area S measured by the tooth imprints (Fig. 5 a) showed that σ is somewhat higher after ultrasonic welding with a coarse tool (Table 3). However, these results are difficult to interpret unambiguously, since during tensile shear tests the weld spot is in a complex stress-strain state [15–17]. Under the action of the tensile force F, shear stresses arise in the plane of the joint, which are balanced by two bending moments. In this case, maximum tensile and compressive stresses arise on the opposite edges (sides) of the weld spot perpendicular to the direction of tension, as shown in Fig. 6. Moreover, a narrow gap – a sharp concentrator located along the perimeter of the weld spot always remains between the overlap-welded plates (Fig. 5 d, e). Attempts are made to take into account the influence of the concentrator on the properties of welded joints, for example, by estimating the value of the critical equivalent stress intensity factor. The results of such an assessment are important in predicting the performance of spot welded joints and structures under the action of cyclic alternating loads and allow partially replacing labour-intensive tests [15; 16]. However, no generally accepted methodology for such assessments has been proposed; different approaches are used [18].

In [15], simple equations were proposed for calculating the critical equivalent stress intensity factor K_{eq} at the tip of a sharp concentrator of spot welded joints–produced by resistance spot welding:

$$K_{eq} = \sqrt{K_I^2 + K_{II}^2} = \frac{\sqrt{19} F_{\max}}{2\pi d \sqrt{h}},$$

where K_I and K_{II} are the stress intensity factors near the tips of the tensile and transverse shear cracks, respectively;
K_{eq} is the critical equivalent stress intensity factor in tensile shear tests;

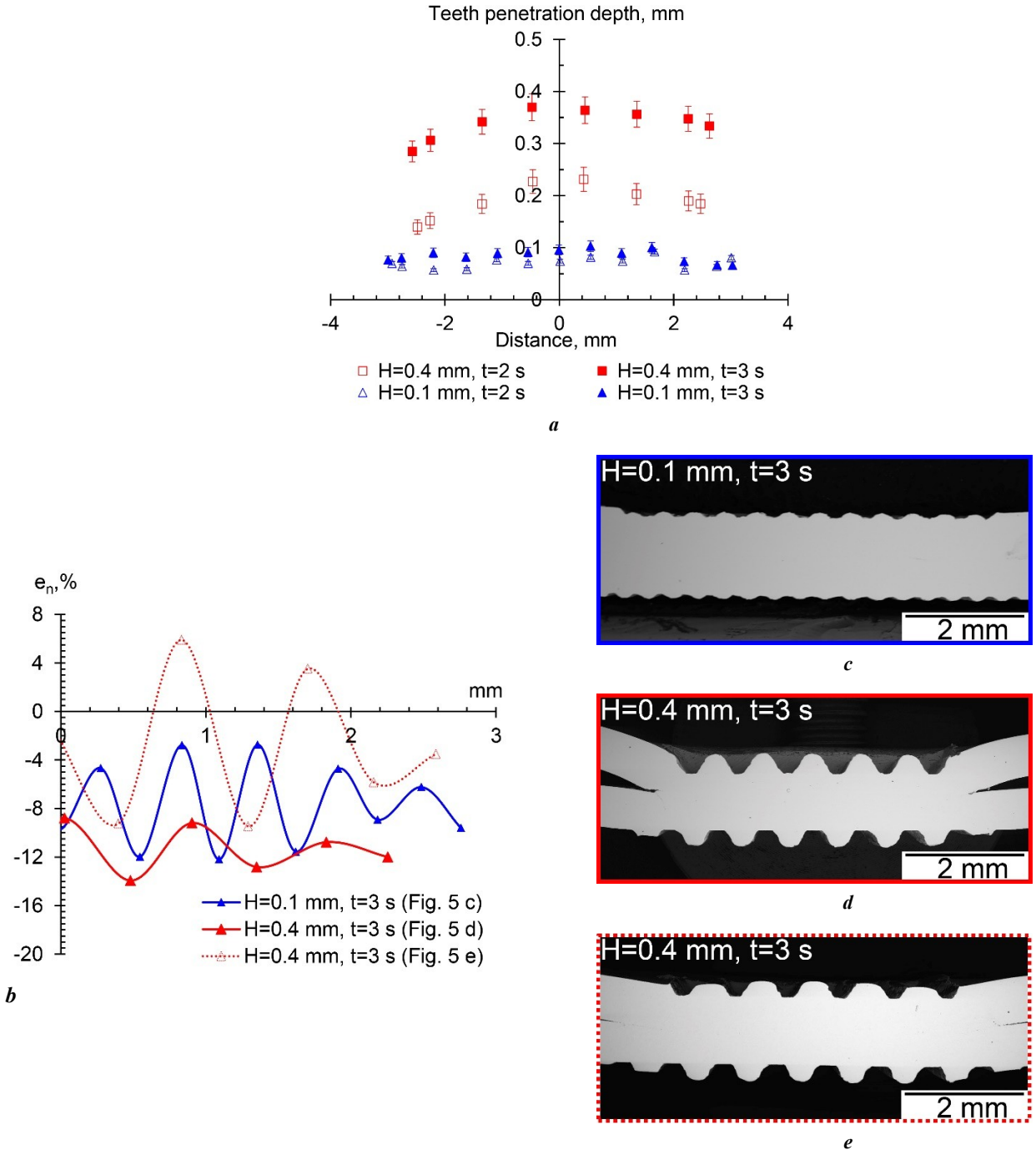

Fig. 5. *Influence of the height of the welding tool teeth on the deformation at the weld spot:*
a *– depth of teeth penetration into the plates being joined;*
b *– distribution of normal deformations of the samples along the joint lines.*
Cross-sections of samples produced by the ultrasonic welding
using the tool with the height of the teeth: ***c*** *– H=0.1 mm;* ***d***, ***e*** *– H=0.4 mm*
Рис. 5. *Влияние высоты зубцов сварочного инструмента на деформацию в сварной точке:*
a *– глубина внедрения наконечника в соединяемые пластины;*
b *– распределение нормальных деформаций образцов вдоль линий соединений.*
Поперечные сечения образцов, полученных УЗС инструментом с высотой зубцов: ***c*** *– H=0,1 мм;* ***d***, ***e*** *– H=0,4 мм*

F_{max} is the maximum loading forces in such tests;
d is the diameter of the weld spot;
h is the thickness of the plates.

This approach has been successfully used to calculate the stress intensity factors arising during testing of joints produced by friction stir spot welding [19; 20] and ultrasonic welding [18; 21–24]. In the latter case, $d=d^*$ is the equivalent diameter of a circle whose area is equal to the area of the weld spot formed by a rectangular welding tip. Obviously, $d^* = \sqrt{4S/\pi}$, where S is the area of the weld spot. When performing assessments,

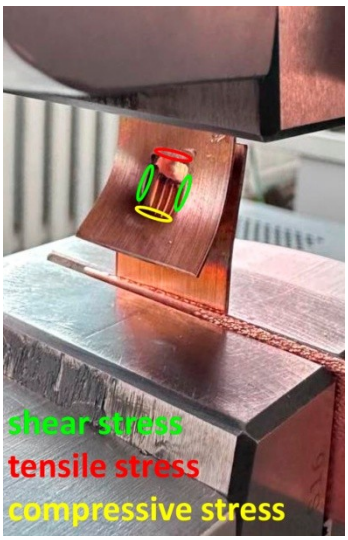

Fig. 6. *Welded sampe in wedge grips of the testing machine during tensile lap shear tests. Scheme of maximum stress distributions near of the welded spot according to [15]*
Рис. 6. *Сварной образец в клиновых захватах машины во время испытаний на сдвиг растяжением. Схема распределения максимальных напряжений вблизи сварной точки по данным [15]*

Table 3. *Initial data and results of the assessment of the critical equivalent stress intensity factor and strength of joints*
Таблица 3. *Исходные данные и результаты оценки критического эквивалентного коэффициента интенсивности напряжений и прочности соединений*

Characteristics of joints	Teeth height (*H*); USW time (*t*)			
	***H*=0.1 mm; *t*=2 s**	***H*=0.1 mm; *t*=3 s**	***H*=0.4 mm; *t*=2 s**	***H*=0.4 mm; *t*=3 s**
S, mm^2	35.21	35.99	24.53	27.03
h, mm	0.71	0.69	0.62	0.49
$\bar{F}_{max}$, N	1593	2075	1814	1918
K_{eq}, MPa√m	6.2	8.1	9.1	10.3
σ, MPa	45	58	74	71

Note. S, mm^2 is a weld spot area;h, mm is the thickness of plates around the weld spot perimeter; $\bar{F}_{max}$ is average values of fracture load; K_{eq} is an equivalent stress intensity factor; σ is the strength of welded joint.
Примечание. S, мм^2 – площадь сварной точки; h, мм – толщина пластин по периметру сварной точки; $\bar{F}_{max}$ – средние значения усилий разрушения;K_{eq} – эквивалентный коэффициент интенсивности напряжений; σ – прочность сварного соединения.

the authors of [21–24] did not take into account the effect of the ultrasonic welding conditions on the size of the weld spot and the change in the plate thickness, taking the area of the spot S to be equal to the area of the welding tip, and the thickness of the plates of the welded sample h to be equal to the thickness of the initial sheet.

Unlike [21–24], in this work, K_{eq} was calculated taking into account changes in S and h, which are caused by the use of a tool with different tooth heights and different USW durations (Table 3). This approach allowed showing that an increase in the welding time with a tool with small and large teeth leads to an increase in the K_{eq} values by approximately 30 and 13 %, respectively. In the first case, the increase in K_{eq} is associated with an increase in $\bar{F}_{max}$, and in the second – with a decrease in the size of the weld spot S and the thickness of the plates h along its edges. A decrease in these geometric dimensions of the samples is accompanied by a rapid decrease in fatigue life [18], despite the increase in critical stresses in the vicinity of the crack tip, causing its rapid propagation. A decrease in h also leads to a change in the fracture mode of the samples, which develops not along the interface of the joint (Fig. 2 a), but with a nugget pull-out (Fig. 2 b, c), and

the crack initiates and grows in the area of action of maximum tensile stresses (Fig. 6).

It is often believed [4; 17] that fracture with nugget pull-out is typical for high-quality joints, since the resistance to the applied load of the welded joint is higher than the cross-section of the plate along its edge. However, even in this case, the microwelds with a developed dimple relief do not cover the entire fracture surface and are located mainly under the tooth imprints (Fig. 4 c). Consequently, the quality of the joints can be improved by optimising the ultrasonic welding parameters and improving the tool relief. For example, some increase in $\bar{F}_{\max}$, $\bar{A}$ and K_{eq} can occur after increasing the clamping force and/or the welding time when welding with a tool with small teeth. However, this will inevitably lead to its accelerated wear. Such measures are not advisable when welding with a tool with large teeth, since they will cause thinning of the plates along the perimeter of the spot. Therefore, improving the relief of the welding tool, taking into account the height of the knurls and the thickness of the plates being joined, seems to be a promising direction for further research.

CONCLUSIONS

The results of a comparative study of joints of 0.8 mm thick copper plates produced by ultrasonic welding at a frequency of 20 kHz and a vibration amplitude of 18–20 μm for 2 and 3 s under the action of a clamping force of 2.5 kN by a tool with a tooth height of 0.1 and 0.4 mm showed that an increase in the ultrasonic welding time to 3 s leads to an increase in the fracture load and fracture energy of the produced joints. The height of the tool teeth did not have a significant effect on the average values of these magnitudes, while the variation coefficient of the experimental values was two times smaller if the ultrasonic welding was performed with a tool with small teeth. Therefore, to improve the stability of the properties of welded joints, it is advisable to use a welding tool with a tooth height of 0.1 mm. After ultrasonic welding with this tool, the weld spot area is larger, and the thinning of the plates is less than after using a tool with 0.4 mm teeth. This can increase the fatigue life, despite the lower values of strength and critical stress intensity factor. However, under the selected USW conditions, its capabilities are not fully realised. To improve the properties of joints and their stability, work is required to further optimise the tool relief and ultrasonic welding modes.

REFERENCES

1. De Leon M., Shin H.S. Review of the advancements in aluminum and copper ultrasonic welding in electric vehicles and superconductor applications. *Journal of Materials Processing Technology*, 2022, vol. 307, article number 117691. DOI: 10.1016/j.jmatprotec.2022.117691.
2. Müller F.W., Mirz C., Schiebahn A., Reisgen U. Influence of quality features, disturbances, sensor data, and measurement time on quality prediction for ultrasonic metal welding. *Welding in the World*, 2025, vol. 69, pp. 1961–1989. DOI: 10.1007/s40194-025-01959-x.
3. Yang Jingwei, Xie Chuhao, Zhang Jie, Qiao Jian. Design strategies for enhancing strength and toughness in ultrasonic welding of dissimilar metals: A review. *Materials Today Communications*, 2025, vol. 42, article number 111502. DOI: 10.1016/j.mtcomm.2025.111502.
4. Yang Jingwei, Cao Diao, Lu Qinghua. The effect of welding energy on the microstructural and mechanical properties of ultrasonic-welded copper joints. *Materials*, 2017, vol. 10, no. 2, article number 193. DOI: 10.3390/ma10020193.
5. Murzinova M.A., Shayakhmetova E.R., Mukhametgalina A.A., Sarkeeva A.A., Nazarov A.A. Local plastic deformation and quality of Cu–Cu joints obtained by ultrasonic welding. *Metals*, 2023, vol. 13, no. 10, article number 1661. DOI: 10.3390/met13101661.
6. Chen Kunkun, Zhang Yansong, Wang Hongze. Study of plastic deformation and interface friction process for ultrasonic welding. *Science and Technology of Welding and Joining*, 2016, vol. 22, no. 3, pp. 208–216. DOI: 10.1080/13621718.2016.1218601.
7. Huang Hui, Chen Jian, Lim Yong Chae, Hu Xiaohua, Cheng Jiahao, Feng Zhili, Sun Xin. Heat generation and deformation in ultrasonic welding of magnesium alloy AZ31. *Journal of Materials Processing Technology*, 2019, vol. 272, pp. 125–136. DOI: 10.1016/j.jmatprotec.2019.05.016.
8. Jedrasiak P., Shercliff H.R. Finite element analysis of heat generation in dissimilar alloy ultrasonic welding. *Materials & Design*, 2018, vol. 158, pp. 184–197. DOI: 10.1016/j.matdes.2018.07.041.
9. Kim Jisun, Kim Jeawoong, Kim Inju. Analysis of welding properties using various horn-tip patterns in the ultrasonic metal welding process. *Mechanics & Industry*, 2020, vol. 21, no. 1, article number 102. DOI: 10.1051/meca/2019078.
10. Du Pengfei, Chen Weishan, Deng Jie, Li Kai, Liu Yingxiang. Effects of knurl tooth angle on mechanical and thermal behaviors of aluminum ultrasonic welding. *Ultrasonics*, 2020, vol. 108, article number 106207. DOI: 10.1016/j.ultras.2020.106207.
11. Ni Z.L., Li B.H., Liu Y., Huang L., Nazarov A., Wang X.X., Yuan Z.P., Ye F.X. Numerical analysis of ultrasonic spot welding of metal sheets: A review. *Science and Technology of Welding and Joining*, 2023, vol. 28, no. 9, pp. 841–864. DOI: 10.1080/13621718.2023.2260625.
12. Mukhametgalina A.A., Murzinova M.A., Nazarov A.A. Microstructure of a titanium sample produced by ultrasonic consolidation. *Letters on materials*, 2022, vol. 12, no. 2, pp. 153–157. DOI: 10.22226/2410-3535-2022-2-153-157.
13. Shayakhmetova E.R., Murzinova M.A., Mukhametgalina A.A., Nazarov A.A. Structure evolution in ultrafine-grained nickel induced by ultrasonic welding. *Letters on materials*, 2024, vol. 14, no. 1, pp. 91–96. DOI: 10.48612/letters/2024-1-91-96.
14. Mukhametgalina A.A., Shayakhmetova E.R., Murzinova M.A., Nazarov A.A., Sarkeeva A.A. Effect of surface state on the quality of copper joints produced by ultrasonic welding. *Letters on materials*, 2024, vol. 14, no. 3, pp. 190–197. DOI: 10.48612/letters/2024-3-190-197.
15. Zhang Shicheng. Stress intensities at spot welds. *International Journal of Fracture*, 1997, vol. 88, pp. 167–185. DOI: 10.1023/A:1007461430066.

16. Zhang Shicheng. Stress intensities derived from stresses around a spot weld. *International Journal of Fracture*, 1999, vol. 99, pp. 239–257. DOI: 10.1023/A:1018608615567.
17. Radakovic D.J., Tumuluru M. Predicting resistance spot weld failure modes in shear tension tests of advanced high-strength automotive steels. *Welding Journal*, 2008, vol. 87, pp. 96s–105s.
18. Patel V.K., Bhole S.D., Chen D.L. Fatigue life estimation of ultrasonic spot welded Mg alloy joints. *Materials & Design*, 2014, vol. 62, pp. 124–132. DOI: 10.1016/j.matdes.2014.05.008.
19. Rosendo T., Tier M., Mazzaferro J., Mazzaferro C., Strohaecker T.R., Dos Santos J.F. Mechanical performance of AA6181 refill friction spot welds under lap shear tensile loading. *Fatigue & Fracture of Engineering Materials & Structures*, 2015, vol. 38, no. 12, pp. 1443–1455. DOI: 10.1111/ffe.12312.
20. Zou Yangfan, Li Wenya, Yang Xiawei et al. Characterizations of dissimilar refill friction stir spot welding 2219 aluminum alloy joints of unequal thickness. *Journal of Manufacturing Processes*, 2022, vol. 79, pp. 91–101. DOI: 10.1016/j.jmapro.2022.04.062.
21. Peng He, Chen Daolun, Jiang Xianguan. Microstructure and mechanical properties of an ultrasonic spot welded aluminum alloy: the effect of welding energy. *Materials*, 2017, vol. 10, no. 5, article number 449. DOI: 10.3390/ma10050449.
22. Mohammed S.M.A.K., Dash S.S., Jiang Xianquan, Li Dongyang, Chen Daolun. Ultrasonic spot welding of 5182 aluminum alloy: evolution of microstructure and mechanical properties. *Materials Science and Engineering: A*, 2019, vol. 56, pp. 417–429. DOI: 10.1016/j.msea.2019.04.059.
23. Ma Qiuchen, Ma Jingyuan, Zhou Jianli, Ji Hongjun. Intrinsic dependence of welding quality and recrystallization on the surface-contacted micro-asperity scale during ultrasonic welding of Cu–Cu joints. *Journal of Materials Research and Technology*, 2022, vol. 17. pp. 353–364. DOI: 10.1016/j.jmrt.2022.01.011.
24. Bajaj D., Mehavarnam R., Fang Xingfan, Ma Ninshu Xu, Li Dongyang, Chen Daolun. Achieving superior aluminum-steel dissimilar joining via ultrasonic spot welding: microstructure and fracture behavior. *Materials Science and Engineering: A*, 2025, vol. 919, article number 147489. DOI: 10.1016/j.msea.2024.147489.

СПИСОК ЛИТЕРАТУРЫ

1. De Leon M., Shin H.S. Review of the advancements in aluminum and copper ultrasonic welding in electric vehicles and superconductor applications // Journal of Materials Processing Technology. 2022. Vol. 307. Article number 117691. DOI: 10.1016/j.jmatprotec.2022.117691.
2. Müller F.W., Mirz C., Schiebahn A., Reisgen U. Influence of quality features, disturbances, sensor data, and measurement time on quality prediction for ultrasonic metal welding // Welding in the World. 2025. Vol. 69. P. 1961–1989. DOI: 10.1007/s40194-025-01959-x.
3. Yang Jingwei, Xie Chuhao, Zhang Jie, Qiao Jian. Design strategies for enhancing strength and toughness in ultrasonic welding of dissimilar metals: A review // Materials Today Communications. 2025. Vol. 42. Article number 111502. DOI: 10.1016/j.mtcomm.2025.111502.
4. Yang Jingwei, Cao Diao, Lu Qinghua. The effect of welding energy on the microstructural and mechanical properties of ultrasonic-welded copper joints // Materials. 2017. Vol. 10. № 2. Article number 193. DOI: 10.3390/ma10020193.
5. Murzinova M.A., Shayakhmetova E.R., Mukhametgalina A.A., Sarkeeva A.A., Nazarov A.A. Local plastic deformation and quality of Cu–Cu joints obtained by ultrasonic welding // Metals. 2023. Vol. 13. № 10. Article number 1661. DOI: 10.3390/met13101661.
6. Chen Kunkun, Zhang Yansong, Wang Hongze. Study of plastic deformation and interface friction process for ultrasonic welding // Science and Technology of Welding and Joining. 2016. Vol. 22. № 3. P. 208–216. DOI: 10.1080/13621718.2016.1218601.
7. Huang Hui, Chen Jian, Lim Yong Chae, Hu Xiaohua, Cheng Jiahao, Feng Zhili, Sun Xin. Heat generation and deformation in ultrasonic welding of magnesium alloy AZ31 // Journal of Materials Processing Technology. 2019. Vol. 272. P. 125–136. DOI: 10.1016/j.jmatprotec.2019.05.016.
8. Jedrasiak P., Shercliff H.R. Finite element analysis of heat generation in dissimilar alloy ultrasonic welding // Materials & Design. 2018. Vol. 158. P. 184–197. DOI: 10.1016/j.matdes.2018.07.041.
9. Kim Jisun, Kim Jeawoong, Kim Inju. Analysis of welding properties using various horn-tip patterns in the ultrasonic metal welding process // Mechanics & Industry. 2020. Vol. 21. № 1. Article number 102. DOI: 10.1051/meca/2019078.
10. Du Pengfei, Chen Weishan, Deng Jie, Li Kai, Liu Yingxiang. Effects of knurl tooth angle on mechanical and thermal behaviors of aluminum ultrasonic welding // Ultrasonics. 2020. Vol. 108. Article number 106207. DOI: 10.1016/j.ultras.2020.106207.
11. Ni Z.L., Li B.H., Liu Y., Huang L., Nazarov A., Wang X.X., Yuan Z.P., Ye F.X. Numerical analysis of ultrasonic spot welding of metal sheets: A review // Science and Technology of Welding and Joining. 2023. Vol. 28. № 9. P. 841–864. DOI: 10.1080/13621718.2023.2260625.
12. Mukhametgalina A.A., Murzinova M.A., Nazarov A.A. Microstructure of a titanium sample produced by ultrasonic consolidation // Letters on materials. 2022. Vol. 12. № 2. P. 153–157. DOI: 10.22226/2410-3535-2022-2-153-157.
13. Shayakhmetova E.R., Murzinova M.A., Mukhametgalina A.A., Nazarov A.A. Structure evolution in ultrafine-grained nickel induced by ultrasonic welding // Letters on materials. 2024. Vol. 14. № 1. P. 91–96. DOI: 10.48612/letters/2024-1-91-96.
14. Mukhametgalina A.A., Shayakhmetova E.R., Murzinova M.A., Nazarov A.A., Sarkeeva A.A. Effect of surface state on the quality of copper joints produced by ultrasonic welding // Letters on materials. 2024. Vol. 14. № 3. P. 190–197. DOI: 10.48612/letters/2024-3-190-197.
15. Zhang Shicheng. Stress intensities at spot welds // International Journal of Fracture. 1997. Vol. 88. P. 167–185. DOI: 10.1023/A:1007461430066.
16. Zhang Shicheng. Stress intensities derived from stresses around a spot weld // International Journal

of Fracture. 1999. Vol. 99. P. 239–257. DOI: 10.1023/A:1018608615567.
17. Radakovic D.J., Tumuluru M. Predicting resistance spot weld failure modes in shear tension tests of advanced high-strength automotive steels // Welding Journal. 2008. Vol. 87. P. 96s–105s.
18. Patel V.K., Bhole S.D., Chen D.L. Fatigue life estimation of ultrasonic spot welded Mg alloy joints // Materials & Design. 2014. Vol. 62. P. 124–132. DOI: 10.1016/j.matdes.2014.05.008.
19. Rosendo T., Tier M., Mazzaferro J., Mazzaferro C., Strohaecker T.R., Dos Santos J.F. Mechanical performance of AA6181 refill friction spot welds under lap shear tensile loading // Fatigue & Fracture of Engineering Materials & Structures. 2015. Vol. 38. № 12. P. 1443–1455. DOI: 10.1111/ffe.12312.
20. Zou Yangfan, Li Wenya, Yang Xiawei et al. Characterizations of dissimilar refill friction stir spot welding 2219 aluminum alloy joints of unequal thickness // Journal of Manufacturing Processes. 2022. Vol. 79. P. 91–101. DOI: 10.1016/j.jmapro.2022.04.062.
21. Peng He, Chen Daolun, Jiang Xianguan. Microstructure and mechanical properties of an ultrasonic spot welded aluminum alloy: the effect of welding energy // Materials. 2017. Vol. 10. № 5. Article number 449. DOI: 10.3390/ma10050449.
22. Mohammed S.M.A.K., Dash S.S., Jiang Xianquan, Li Dongyang, Chen Daolun. Ultrasonic spot welding of 5182 aluminum alloy: evolution of microstructure and mechanical properties // Materials Science and Engineering: A. 2019. Vol. 56. P. 417–429. DOI: 10.1016/j.msea.2019.04.059.
23. Ma Qiuchen, Ma Jingyuan, Zhou Jianli, Ji Hongjun. Intrinsic dependence of welding quality and recrystallization on the surface-contacted micro-asperity scale during ultrasonic welding of Cu–Cu joints // Journal of Materials Research and Technology. 2022. Vol. 17. P. 353–364. DOI: 10.1016/j.jmrt.2022.01.011.
24. Bajaj D., Mehavarnam R., Fang Xingfan, Ma Ninshu Xu, Li Dongyang, Chen Daolun. Achieving superior aluminum-steel dissimilar joining via ultrasonic spot welding: microstructure and fracture behavior // Materials Science and Engineering: A. 2025. Vol. 919. Article number 147489. DOI: 10.1016/j.msea.2024.147489.

УДК 534-8; 621.791.16
doi: 10.18323/2782-4039-2025-3-73-10

Прочность соединений пластин меди, полученных точечной ультразвуковой сваркой инструментом с разной высотой зубцов

Шаяхметова Эльвина Рафитовна, младший научный сотрудник
Институт проблем сверхпластичности металлов РАН, Уфа (Россия)

E-mail: elvinar@imsp.ru ORCID: https://orcid.org/0000-0002-1659-9922

Поступила в редакцию 30.06.2025 *Пересмотрена 21.07.2025* *Принята к публикации 12.08.2025*

Аннотация: Ультразвуковая сварка (УЗС) металлов позволяет получать твердофазные соединения между тонкими заготовками и относится к энергоэффективным экологически чистым технологиям. Широкое использование этой технологии сдерживает невысокая прочность получаемых соединений и нестабильность их свойств. Одним из способов повышения прочностных характеристик является разработка сварочного инструмента, обеспечивающего стабильную передачу энергии ультразвуковых колебаний в зону соединения. Для этого на поверхность сварочного наконечника и наковальни наносят рельеф с зубцами или пирамидками разной формы и высоты. В работе представлены данные об усилиях и работе разрушения нахлесточных соединений, полученных точечной ультразвуковой сваркой пластин меди инструментом с высотой зубцов 0,1 и 0,4 мм. УЗС проводили с частотой 20 кГц и амплитудой колебаний 18–20 мкм, длительность сварки составляла 2 и 3 с, величина сжимающей нагрузки 2,5 кН. В работе рассмотрены особенности разрушения полученных соединений и распределения нормальных деформаций в сварной точке, рассчитаны коэффициенты интенсивности напряжений в ее окрестностях. Показано, что после УЗС в течение 3 с показатели прочности соединений, полученных разным инструментом, достигают наибольших значений, они близки по величине, однако разброс экспериментальных данных вдвое меньше после сварки инструментом с мелкими зубцами. Соединения, полученные таким инструментом, разрушаются по поверхности соединения, а после сварки инструментом с крупными зубцами – с отрывом сварной точки, что объясняется увеличением коэффициента интенсивности напряжений в вершине концентратора, окружающего сварную точку.

Ключевые слова: медь; ультразвуковая сварка металлов; твердофазное соединение; прочность соединений; рельеф сварочного инструмента; коэффициент интенсивности напряжений.

Благодарности: Исследование выполнено в рамках государственного задания ИПСМ РАН (регистрационный номер 124022900006-2). Часть экспериментальных данных получена при выполнении гранта РНФ № 22-19-00617

(https://rscf.ru/project/22-19-00617/). Микроструктурные исследования проводились на базе ЦКП ИПСМ РАН «Структурные и физико-механические исследования материалов».

Автор выражает глубокую благодарность к.т.н. М.А. Мурзиновой и д.ф.-м.н. А.А. Назарову за помощь при проведении исследований и обсуждение полученных результатов.

Статья подготовлена по материалам докладов участников XII Международной школы «Физическое материаловедение» (ШФМ-2025), Тольятти, 15–19 сентября 2025 года.

Для цитирования: Шаяхметова Э.Р. Прочность соединений пластин меди, полученных точечной ультразвуковой сваркой инструментом с разной высотой зубцов // Frontier Materials & Technologies. 2025. № 3. С. 125–136. DOI: 10.18323/2782-4039-2025-3-73-10.